

How good are recent density functionals for ground and excited states of one-electron systems?

Sebastian Schwalbe,^{1, a)} Kai Trepte,^{2, b)} and Susi Lehtola^{3, c)}

¹⁾*Institute of Theoretical Physics, TU Bergakademie Freiberg, D-09599 Freiberg, Germany*

²⁾*Taiwan Semiconductor Manufacturing Company North America, San Jose, CA 95134, USA*

³⁾*Molecular Sciences Software Institute, Blacksburg, VA 24061, USA*

(Dated: 9 November 2022)

Sun et al. [J. Chem. Phys. 144, 191101 (2016)] suggested that common density functional approximations (DFAs) should exhibit large energy errors for excited states as a necessary consequence of orbital nodality. Motivated by self-interaction corrected density functional calculations on many-electron systems, we continue their study with the exactly solvable $1s$, $2p$, and $3d$ states of 36 hydrogenic one-electron ions (H-Kr^{35+}) and demonstrate with self-consistent calculations that state-of-the-art DFAs indeed exhibit large errors for the $2p$ and $3d$ excited states. We consider 56 functionals at the local density approximation (LDA), generalized gradient approximation (GGA) as well as meta-GGA levels, also including several hybrid functionals like the recently proposed machine-learned DM21 local hybrid functional. The best non-hybrid functional for the $1s$ ground state is revTPSS. The $2p$ and $3d$ excited states are more difficult for DFAs as Sun et al. predicted, and LDA functionals turn out to yield the most systematic accuracy for these states amongst non-hybrid functionals. The best performance for the three states overall is observed with the BHandH global hybrid GGA functional, which contains 50% Hartree–Fock exchange and 50% LDA exchange. The performance of DM21 is found to be inconsistent, yielding good accuracy for some states and systems and poor accuracy for others. Based on these results, we recommend including a variety of one-electron cations in future training of machine-learned density functionals.

I. INTRODUCTION

Density-functional theory^{1,2} (DFT) has become one of the workhorses of computational chemistry, material science, and related fields, as modern density functional approximations (DFAs) only require a reasonable amount of computational effort while providing a level of accuracy sufficient for semi-quantitative predictions on a broad range of systems.^{3–5} Although hundreds of DFAs have been proposed, thus forming the infamous zoo of DFAs,⁶ new DFAs continue to be developed in the aim to find more universally applicable DFAs that combine suitable levels of accuracy and numerical effort.

New DFAs can be constructed along various strategies.^{5,7–9} The traditional route to construct DFAs is to start from first principles and to impose known limits and constraints; this is the way along which many well-known functionals such as PBE¹⁰, TPSS^{11,12}, and SCAN¹³ have been constructed.

Semi-empirical fitting is another route for constructing DFAs. Here, the general idea is to introduce flexibility in the functional form by introducing several independent DFA components that are weighted by parameters which are optimized against some training dataset. Classical examples of semi-empirically fitted functionals include B3LYP,¹⁴ Becke’s 1997 functional¹⁵ (B97) and several refinements thereof such as the HCTH [Hamprecht–Cohen–Tozer–Handy] functionals by Handy and coworkers,^{16,17}

as well as the Minnesota family of DFAs by Truhlar and coworkers^{18,19} that has been reviewed by Mardirossian and Head-Gordon²⁰.

In reality, the classification of functionals into ones built solely from first principles vs ones formed by semi-empirical fitting is not always clear: for instance, the TPSS exchange functional is parametrized to yield the exact energy for the hydrogen atom’s exact ground state density,^{11,12} while the SCAN functional¹³ includes parameters that are fit to data on noble gases. Modern semi-empirical functionals,^{21–26} in turn, typically employ a combination of the two approaches by restricting the fits to known constraints.

DFAs from either route are widely used, given their suitable numerical accuracy and reasonable computational effort. However, the functionals obtained from the two routes tend to exhibit different behavior. For instance, while semi-empirical DFAs often deliver excellent descriptions of the total energy, they may fail to reproduce electronic densities of the same quality: a famous article of Medvedev *et al.*²⁷ initiated an intense debate about this in the literature,^{27–32}; it was even pointed out that any general mathematical measure of density error is too arbitrary to be universally useful.³³ DFAs built on physical first principles, in contrast, often yield steady performance in a variety of applications, but may not achieve the same level of accuracy as tailored functionals for specific types of systems.

One of the most important limitations of present-day DFAs, regardless of their design, is the self-interaction error (SIE): an artificial interaction of the electrons with themselves. This error is related to density delocalization error and the fractional electron problem,^{34,35} and leads

^{a)}Electronic mail: schwalbe@physik.tu-freiberg.de

^{b)}Electronic mail: kai.trepte1987@gmail.com

^{c)}Electronic mail: susi.lehtola@alumni.helsinki.fi

to incorrect dissociation limits³⁶ and barrier heights,³⁷ for instance. Recent avenues for circumventing SIE in DFAs involve determining the electron density with another method, such as Hartree–Fock^{38,39} or multiconfigurational wave function theory^{40,41}. Other types of approaches have also been proposed in the literature. To solve the self-interaction problem, Perdew and Zunger⁴² (PZ) proposed an orbital-by-orbital self-interaction correction (SIC)

$$E^{\text{PZ}} = E^{\text{KS}} - \sum_{i\sigma} \Delta_{i\sigma}, \quad (1)$$

where E^{KS} is the Kohn–Sham (KS) energy functional² and the self-interaction error (SIE) is defined by

$$\Delta_{i\sigma} = E_J[n_{i\sigma}] + E_{\text{xc}}[n_{i\sigma}]. \quad (2)$$

Here, $n_{i\sigma}$ is the electron density of the i -th occupied orbital with spin σ and E_J and E_{xc} denote the Coulomb and exchange–correlation energy functionals, respectively. The idea behind PZ-SIC is that the self-interaction error defined by equation (2) vanishes for the exact functional,⁴² and thereby the Perdew–Zunger functional of equation (1) is a better estimate for the total energy than the uncorrected Kohn–Sham DFA E^{KS} ; indeed, the PZ functional is exact for one-electron systems such as the H_2^+ molecule with approximate DFAs.

Despite the simple logic used to construct the PZ-SIC functional, the PZ-SIC method turns out to be quite complicated. The introduction of the explicit orbital dependence in equations (1) and (2) breaks the unitary invariance of the energy functional,⁴³ requiring costly unitary optimization of the orbitals (see Ref. 44 for discussion). However, even though the resulting method is known to correct charge transfer errors and barrier heights, it does not lead to improved atomization energies with GGA and meta-GGA functionals in general.⁴⁵

Continued research has illuminated other important theoretical aspects of PZ-SIC. First, the orbital dependence in equations (1) and (2) has been recently shown to require the use of complex-valued orbitals for proper minimization, as real-valued orbitals can be shown to correspond to high-order saddle points.⁴⁶ When complex-valued orbitals are employed, the total energy is lowered, and PZ-SIC does lead to improved atomization energies for some GGA functionals; however, more accurate atomization energies can be obtained at significantly smaller cost with several standard DFAs.⁴⁷

Second, the orbital dependence in equations (1) and (2) has also been shown to lead to the existence of several local minima in the orbital space.⁴⁶ This problem has been recently shown to persist also in a related SIC method⁴⁸ based on the use of Fermi–Löwdin orbitals (PZFLO-SIC), where various choices for the orbital descriptors lead to distinct local electronic minima.⁴⁹ The existence of such local minima is a significant and underappreciated aspect of PZ-SIC and PZFLO-SIC calculations, as finding the true ground state may require extensive sampling of the

space of the various possible localized electronic configurations or bonding situations.

Despite their theoretical shortcomings, PZ-SIC and PZFLO-SIC have been found useful in many applications^{50–52} and we are positive that several of the aforementioned issues in PZ-SIC and PZFLO-SIC can be addressed by developments in the related theories by changing the way the self-interaction correction is applied. One possible way to achieve improved results would be to revisit DFAs based on the requirements of SIC calculations.⁵³ It is known that present-day DFAs yield poor estimates for the noded electron densities that are involved in SIC calculations.^{54,55} Sun *et al.*⁵⁴ demonstrated that the ground and excited state densities of the hydrogen atom (as well as of H_2^+ , see below) lead to large relative errors in the exchange–correlation energy compared to the exact values, but we are not aware of any self-consistent calculations on this issue.

Following recent discussion in the literature on the accuracy of DFAs on the electron densities of small atoms and ions^{27–33} and motivated by the obvious connection of one-electron errors (OEEs) to the PZ-SIC and PZFLO-SIC methods, in this work we will analyze the OEE of various functionals for the $1s$ ground state as well as the $2p$ and $3d$ excited states of hydrogenic ions $Z^{(Z-1)+}$, whose exact energies are well-known to be given in atomic units by

$$E_n = -Z^2/2n^2, \quad (3)$$

where Z is the atomic number, $n \geq l + 1$ is the principal quantum number, and l is the angular momentum.

As was mentioned above, calculations of ground and excited states of the hydrogen atom and of the $1\sigma_g$ ground state and $1\sigma_u$ excited state of H_2^+ have been discussed by Sun *et al.*⁵⁴ with non-self-consistent electron densities, while the $1s$ ground states of hydrogenic mononuclear cations as well as the 1σ ground states of hydrogenic diatomic cations have been discussed recently by Lonsdale and Goerigk⁵⁶ using self-consistent calculations. The novel contribution of this work is to address (highly) excited states with noded electron densities of hydrogenic cations self-consistently. Importantly, like the $1s$ ground state, the $2p$ and $3d$ excited states (as well as the analogous higher excited states like $4f$) are the lowest states of the corresponding symmetry, and the ground-state Kohn–Sham scheme is applicable to such excited states as well as shown by Gunnarsson and Lundqvist⁵⁷.

We pursue thorough density functional investigations of the $1s$, $2p$, and $3d$ states of hydrogenic ions in benchmark-quality Gaussian basis sets specially suited for this purpose with a selection of 56 popular DFAs, including the recently developed, highly sophisticated machine-learned DeepMind 21 (DM21) local hybrid functional.⁵⁸

The layout of this work is as follows. The computational details are presented in section §II, and the results are given in section §III. A summary of our findings and an outlook for further investigations is given in

section §IV. Atomic units are used throughout, unless specified otherwise.

II. COMPUTATIONAL DETAILS

We only use free and open-source software (FOSS) in this work, following the philosophy discussed in Ref. 59. PYSCF⁶⁰ is an electronic structure code for all-electron calculations using Gaussian-type orbitals (GTOs). As we are targeting one-electron states of specific symmetry (s , p , or d states), following Gunnarsson and Lundqvist⁵⁷ we truncate the basis set in all calculations to contain functions only of the pursued symmetry: calculations on the $1s/2p/3d$ state only include the basis functions of the corresponding symmetry (s , p , or d functions, respectively) from the chosen parent basis set. This procedure has two important features: the $2p$ and $3d$ excited states become the ground state in the reduced-basis calculation, and the computational requirements are smaller since fewer integrals need to be calculated in the reduced basis than in the original basis set.

The one-electron guess—which is exact for one-electron systems and thereby is also expected to be accurate for calculations employing DFAs as well—is used in all calculations.⁶¹ To ensure that the SCF procedure converges to the global minimum instead of a saddle point, the following procedure was used. First, a regular SCF calculation was performed with PYSCF with default settings; direct inversion in the iterative subspace (DIIS) is used to accelerate these calculations.^{62,63} Next, convergence to saddle point solutions was checked: cases where the SCF converged to a final energy higher than that of the initial guess were restarted, with new calculations employing iterative diagonalization with level shifting⁶⁴ instead of DIIS to converge to the ground state. All calculations reported in this work are fully converged to a threshold of $1 \times 10^{-7} E_h$.

For the GTO basis sets, we use the family of hydrogenic Gaussian basis sets⁶⁵ (HGBS- n) that have been designed for high-accuracy calculations on atoms and small molecules. A special feature of the HGBS basis sets is that the basis for atomic number Z is determined by a universal even-tempered basis set for the ions $Y^{(Y-1)+}$ for $Y \in [1, Z]$, whereas augmented hydrogenic Gaussian basis sets (AHGBS- n) add further functions for describing the $Z = 0.5$ one-electron ion.⁶⁵ The parameter n controls the relative precision of the hydrogenic Gaussian basis; (A)HGBS- n reproduces the exact total energies of the one-electron ions to an approximate relative accuracy of 10^{-n} .⁶⁵ The motivation of this approach in Ref. 65 was that a many-electron atom experiences a screened nuclear charge that can be rewritten in terms of a radially dependent effective charge $Z^{\text{eff}} = Z^{\text{eff}}(r)$ with the asymptotic limits $Z^{\text{eff}}(0) = Z$ and either $Z^{\text{eff}}(\infty) = Z_\infty$ with the asymptotic limit $Z_\infty = 0$ for Hartree–Fock and DFT or $Z_\infty = 1$ for the exact effective potential.⁶¹

Another feature of the HGBS basis sets is that the

functions of various angular symmetries are determined independently of each other, which facilitates the formation of polarized counterparts of the basis sets that are essential for studying molecules and excited states, as additional shells are added to the basis like lego blocks.⁶⁵ Following Ref. 65, the basis set with $p \geq 1$ polarization shells and accuracy n is denoted (A)HGBSP p - n . The definition of polarization shells varies by atom (see Ref. 65 for discussion); however, as we only include the functions of the pursued symmetry in each calculation, the choice of the polarization level of the (A)HGBSP p - n basis set does not matter as long as the original basis contains functions of the highest targeted angular momentum for the targeted atom, that is, d functions in this work.

For the reasons listed above, the hydrogenic Gaussian basis sets of Ref. 65 are ideally suited for the present study—as will be demonstrated in section §III by benchmarks with functions from the polarization consistent (pc- n) basis sets⁶⁶ and their augmented versions⁶⁷ (aug-pc- n)—and, as will be discussed in section §III A, we will take the exponents from the AHGBSP3- n basis sets in this work. All basis sets were taken from the Basis Set Exchange.⁶⁸

The LIBXC library⁹—which implements over 600 DFAs—is used in PYSCF to evaluate the DFAs. The library provides access to a vast variety of DFAs, of which 49 were chosen for this work; see table 1 for the complete list of investigated functionals. Our selection includes functionals of the first to the fourth rung of Jacob’s ladder,¹²³ that is, local density approximations (LDAs), generalized gradient approximations (GGAs), meta-GGAs, as well as global and range-separated hybrid functionals. In addition, we consider six hybrids of rSCAN and r²SCAN with varying fractions of Hartree–Fock exchange discussed in Ref. 120; these functionals were defined in the PYSCF input files as weighted combinations of r(²)SCAN exchange and Hartree–Fock exchange + 100% r(²)SCAN correlation. The DM21 functional was also chosen for this study; we use the original implementation in PYSCF of Kirkpatrick *et al.*⁵⁸. This brings up the total to 56 functionals for this study. An unpruned (300,590) quadrature grid is used in all calculations, including the non-local correlation component in B97M-V, ω B97M-V and LC-VV10.

As the total energies scale as $E_n \propto Z^2$ according to equation (3), the results will be analyzed in terms of absolute relative errors (AREs). Hydrogenic estimates show that the approximated exchange-correlation energy scales like Z in the large Z limit,¹²⁴ meaning that the relative errors should tend to zero like $1/Z$. The ARE for a given state of a given ion is given by

$$\text{ARE} = |(E_{\text{calc}} - E_{\text{ref}})/E_{\text{ref}}|. \quad (4)$$

The information in the AREs is analyzed with two further error metrics. The mean state error (MSE) measures the overall functional error over all ions by averaging the

Table 1. List of investigated functionals, including the publication year, the LIBXC identifier, the calculated MSEs for the $1s$, $2p$, and $3d$ states as well as the respective OE. Tables containing functional rankings by error for the individual states as well as the OE can be found in the supplementary material (Tables S1–S4). The Libxc identifiers contain information about the functional; in addition to the rung of Jacob’s ladder: LDA, GGA, or meta-GGA (mGGA), hybrid (hyb) functionals are also identifiable from the list.

Name	Year	LIBXC identifier	MSE			OE
			$1s$	$2p$	$3d$	
ω B97M-V ²³	2016	HYB_MGGA_XC_WB97M_V	8.106×10^{-4}	5.987×10^{-3}	1.128×10^{-2}	6.027×10^{-3}
ω B97X-D ⁶⁹	2008	HYB_GGA_XC_WB97X_D	7.641×10^{-4}	1.385×10^{-2}	2.512×10^{-2}	1.324×10^{-2}
B3LYP ^{14,70–73}	1994	HYB_GGA_XC_B3LYP	7.203×10^{-4}	1.055×10^{-2}	2.464×10^{-2}	1.197×10^{-2}
B97-1 ¹⁶	1998	HYB_GGA_XC_B97_1	3.756×10^{-4}	1.108×10^{-2}	2.436×10^{-2}	1.194×10^{-2}
B97M-V ²²	2015	MGGA_XC_B97M_V	2.466×10^{-4}	5.258×10^{-3}	1.491×10^{-2}	6.804×10^{-3}
BHandH ⁷³	1993	HYB_GGA_XC_BHANDH	5.122×10^{-3}	2.822×10^{-3}	4.341×10^{-4}	2.793×10^{-3}
BLOC ^{74,75}	2013	MGGA_X_BLOC, MGGA_C_REVTPSS	2.046×10^{-5}	1.094×10^{-2}	2.320×10^{-2}	1.139×10^{-2}
BLYP ^{70–72}	1988	GGA_X_B88, GGA_C_LYP	5.790×10^{-4}	1.209×10^{-2}	2.857×10^{-2}	1.374×10^{-2}
BLYP35 ^{76,77}	2011	HYB_GGA_XC_BLYP35	3.902×10^{-4}	7.824×10^{-3}	1.837×10^{-2}	8.861×10^{-3}
BOP ^{70,78}	1999	GGA_X_B88, GGA_C_OP_B88	5.789×10^{-4}	1.209×10^{-2}	2.857×10^{-2}	1.374×10^{-2}
CAM-B3LYP ⁷⁹	2004	HYB_GGA_XC_CAM_B3LYP	8.286×10^{-4}	7.569×10^{-3}	1.617×10^{-2}	8.188×10^{-3}
CAM-QTP00 ⁸⁰	2014	HYB_GGA_XC_CAM_QTP_00	4.572×10^{-4}	4.187×10^{-3}	8.300×10^{-3}	4.315×10^{-3}
CAM-QTP01 ⁸¹	2016	HYB_GGA_XC_CAM_QTP_01	1.339×10^{-3}	4.961×10^{-3}	9.542×10^{-3}	5.281×10^{-3}
CAM-QTP02 ⁸²	2018	HYB_GGA_XC_CAM_QTP_02	1.714×10^{-3}	3.302×10^{-3}	6.680×10^{-3}	3.899×10^{-3}
CHACHIYO ^{83,84}	2015	LDA_X, LDA_C_CHACHIYO	7.711×10^{-3}	3.476×10^{-3}	1.155×10^{-2}	7.579×10^{-3}
DM21 ⁵⁸	2021	Uses PySCF implementation instead of LIBXC	2.126×10^{-3}	5.435×10^{-3}	1.226×10^{-2}	6.606×10^{-3}
GAM ⁸⁵	2015	GGA_X_GAM, GGA_C_GAM	2.584×10^{-3}	1.561×10^{-2}	3.650×10^{-2}	1.823×10^{-2}
HCTH-93 ¹⁶	1998	GGA_X_HCTH_93	9.252×10^{-4}	1.642×10^{-2}	3.689×10^{-2}	1.808×10^{-2}
HSE03 ^{86,87}	2003	HYB_GGA_XC_HSE03	1.116×10^{-3}	1.150×10^{-2}	2.453×10^{-2}	1.238×10^{-2}
HSE06 ^{86–88}	2006	HYB_GGA_XC_HSE06	6.659×10^{-4}	8.785×10^{-3}	2.052×10^{-2}	9.989×10^{-3}
HSE12 ⁸⁹	2012	HYB_GGA_XC_HSE12	6.187×10^{-4}	8.201×10^{-3}	1.911×10^{-2}	9.309×10^{-3}
LC-QTP ⁸²	2018	HYB_GGA_XC_LC_QTP	2.276×10^{-3}	3.818×10^{-3}	7.590×10^{-3}	4.561×10^{-3}
LC-VV10 ⁹⁰	2010	HYB_GGA_XC_LC_VV10	1.089×10^{-3}	6.905×10^{-3}	1.166×10^{-2}	6.553×10^{-3}
LRC- ω PBE ⁹¹	2009	HYB_GGA_XC_LRC_WPBE	1.121×10^{-3}	9.294×10^{-3}	1.668×10^{-2}	9.033×10^{-3}
M06-L ^{92,93}	2006	MGGA_X_M06_L, MGGA_C_M06_L	9.242×10^{-4}	1.521×10^{-2}	3.368×10^{-2}	1.660×10^{-2}
M11-L ⁹⁴	2012	MGGA_X_M11_L, MGGA_C_M11_L	2.320×10^{-3}	1.876×10^{-2}	4.593×10^{-2}	2.234×10^{-2}
MN12-L ⁹⁵	2012	MGGA_X_MN12_L, MGGA_C_MN12_L	1.541×10^{-3}	5.796×10^{-3}	2.036×10^{-2}	9.234×10^{-3}
MN15 ⁹⁶	2016	HYB_MGGA_X_MN15, MGGA_C_MN15	2.532×10^{-4}	9.867×10^{-3}	2.133×10^{-2}	1.048×10^{-2}
MN15-L ⁹⁷	2016	MGGA_X_MN15_L, MGGA_C_MN15_L	2.118×10^{-3}	4.673×10^{-3}	1.327×10^{-2}	6.689×10^{-3}
MS0 ^{98–100}	2012	MGGA_X_MS0, GGA_C_REGTPSS	5.973×10^{-4}	1.121×10^{-2}	2.233×10^{-2}	1.138×10^{-2}
MS1 ^{99–101}	2013	MGGA_X_MS1, GGA_C_REGTPSS	6.013×10^{-4}	1.161×10^{-2}	2.346×10^{-2}	1.189×10^{-2}
MS2 ^{99–101}	2013	MGGA_X_MS2, GGA_C_REGTPSS	6.039×10^{-4}	1.193×10^{-2}	2.432×10^{-2}	1.229×10^{-2}
OLYP ^{71,102}	2009	GGA_X_OPTX, GGA_C_LYP	3.934×10^{-4}	1.309×10^{-2}	2.971×10^{-2}	1.440×10^{-2}
PBE ^{10,103}	1996	GGA_X_PBE, GGA_C_PBE	9.196×10^{-4}	1.096×10^{-2}	2.538×10^{-2}	1.242×10^{-2}
PBEsol ¹⁰⁴	2007	GGA_X_PBE_SOL, GGA_C_PBE_SOL	3.799×10^{-3}	6.918×10^{-3}	2.010×10^{-2}	1.027×10^{-2}
PKZB ¹⁰⁵	1999	MGGA_X_PKZB, MGGA_C_PKZB	9.408×10^{-4}	1.038×10^{-2}	2.470×10^{-2}	1.201×10^{-2}
PW91 ^{106–108}	1992	GGA_X_PW91, GGA_C_PW91	7.771×10^{-4}	1.086×10^{-2}	2.449×10^{-2}	1.204×10^{-2}
QTP17 ¹⁰⁹	2018	HYB_GGA_XC_QTP17	3.060×10^{-3}	1.483×10^{-3}	4.612×10^{-3}	3.051×10^{-3}
RPBE ^{10,103,110}	1999	GGA_X_RPBE, GGA_C_PBE	4.576×10^{-4}	1.346×10^{-2}	2.932×10^{-2}	1.441×10^{-2}
SPW92 ^{83,111}	1992	LDA_X, LDA_C_PW_MOD	7.702×10^{-3}	3.392×10^{-3}	1.138×10^{-2}	7.490×10^{-3}
SVWN ^{83,112,113}	1980	LDA_X, LDA_C_VWN	7.707×10^{-3}	3.390×10^{-3}	1.138×10^{-2}	7.492×10^{-3}
TASK ^{111,114}	2019	MGGA_X_TASK, LDA_C_PW	2.523×10^{-3}	1.463×10^{-2}	2.698×10^{-2}	1.471×10^{-2}
TM ¹¹⁵	2016	MGGA_X_TM, MGGA_C_TM	2.972×10^{-5}	1.035×10^{-2}	2.240×10^{-2}	1.093×10^{-2}
TPSS ^{11,12}	2003	MGGA_X_TPSS, MGGA_C_TPSS	2.046×10^{-5}	1.094×10^{-2}	2.318×10^{-2}	1.138×10^{-2}
TPSSH ¹¹⁶	2003	HYB_MGGA_XC_TPSSH	1.640×10^{-5}	9.835×10^{-3}	2.080×10^{-2}	1.022×10^{-2}
XLYP ¹¹⁷	2004	GGA_XC_XLYP	1.369×10^{-4}	1.217×10^{-2}	2.792×10^{-2}	1.341×10^{-2}
r ² SCAN ^{118,119}	2020	MGGA_X_R2SCAN, MGGA_C_R2SCAN	1.495×10^{-5}	8.087×10^{-3}	1.617×10^{-2}	8.091×10^{-3}
r ² SCAN0 ¹²⁰	2022	Custom-defined in PySCF	8.173×10^{-6}	6.051×10^{-3}	1.204×10^{-2}	6.035×10^{-3}
r ² SCAN50 ¹²⁰	2022	Custom-defined in PySCF	3.504×10^{-6}	4.025×10^{-3}	7.975×10^{-3}	4.001×10^{-3}
r ² SCANh ¹²⁰	2022	Custom-defined in PySCF	1.198×10^{-5}	7.271×10^{-3}	1.451×10^{-2}	7.266×10^{-3}
rSCAN ¹²¹	2019	MGGA_X_RSCAN, MGGA_C_RSCAN	1.495×10^{-5}	8.087×10^{-3}	1.617×10^{-2}	8.091×10^{-3}
rSCAN0 ¹²⁰	2022	Custom-defined in PySCF	8.173×10^{-6}	6.051×10^{-3}	1.204×10^{-2}	6.034×10^{-3}
rSCAN50 ¹²⁰	2022	Custom-defined in PySCF	3.504×10^{-6}	4.025×10^{-3}	7.975×10^{-3}	4.001×10^{-3}
rSCANh ¹²⁰	2022	Custom-defined in PySCF	1.198×10^{-5}	7.271×10^{-3}	1.451×10^{-2}	7.266×10^{-3}
revPBE ^{10,103,122}	1998	GGA_X_PBE_R, GGA_C_PBE	4.572×10^{-4}	1.358×10^{-2}	2.995×10^{-2}	1.466×10^{-2}
revTPSS ^{99,100}	2009	MGGA_X_REVTPSS, MGGA_C_REVTPSS	1.302×10^{-5}	1.040×10^{-2}	2.186×10^{-2}	1.076×10^{-2}

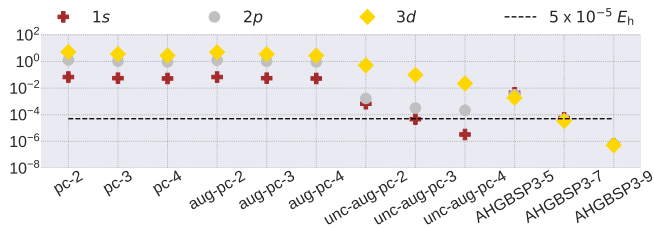


Figure 1. Mean basis set truncation error (ME) in E_h at UHF level of theory for the $1s$ ground state and the $2p$ and $3d$ excited states, respectively. The reference values are calculated with equation (3), and the aimed accuracy threshold $5 \times 10^{-5} E_h$ is shown with the dashed horizontal line.

ARE over all ions

$$\text{MSE} = 1/N_{\text{ions}} \sum_i^{N_{\text{ions}}} \text{ARE}_i. \quad (5)$$

The overall error (OE) for a functional is obtained by further averaging the MSE over all considered states ($1s$, $2p$, and $3d$)

$$\text{OE} = 1/N_{\text{states}} \sum_i^{N_{\text{states}}} \text{MSE}_i. \quad (6)$$

III. RESULTS

A. Basis set convergence

Before pursuing density functional calculations, we analyze the basis set truncation errors (BSTEs) for the one-electron cations in the polarization consistent and hydrogenic Gaussian basis sets. We aim for a mean BSTE smaller than $5 \times 10^{-5} E_h$ for the whole benchmark set ranging from H^0 to Kr^{35+} to ensure that our results are converged close to the complete basis set limit.

Unrestricted Hartree–Fock (UHF) is exact for one-electron systems and thereby gives the exact energy E_n^{UHF} in the studied basis; the difference of $E_n^{\text{UHF}/\text{basis}}$ and the exact analytical energy (equation (3))

$$\Delta_n^{\text{basis}} = E_n^{\text{UHF}/\text{basis}} - E_n \geq 0 \quad (7)$$

is therefore a variational measure of the BSTE for the state with given n of the studied hydrogenic ions.

The calculated mean BSTEs for a variety of polarization consistent and hydrogenic Gaussian basis sets are shown in figure 1; additional results can be found in the supplementary material. Unsurprisingly, uncontracting the (aug-)pc- n basis sets—yielding the unc-(aug-)pc- n basis sets—results in a noticeable decrease of the BSTE, because the contractions were determined in Ref. 66 with the BLYP functional^{70–72} that suffers from SIE for the $1s$ state, while the p and d functions in the basis set describe

either polarization effects or the occupied p or d orbitals in the screened neutral atom. Although the large uncontracted polarization consistent basis sets exhibit satisfactory performance for the $1s$ state, they result in much larger errors for the $2p$ and $3d$ states; this error is again caused by the p and d orbitals in the neutral atom being screened by the core electrons, which results in the lack of tight p and d basis functions that are necessary for the $2p$ and $3d$ states of the one-electron ions.

In contrast, the primitive (not contracted) hydrogenic Gaussian basis sets of Ref. 65 show uniform accuracy for the $1s$, $2p$, and $3d$ states, and as can be observed in figure 1, the targeted mean BSTE threshold is roughly achieved already with the AHGBSP3-7 basis set. The AHGBSP3-9 basis sets yield errors below the desired threshold for all states, and is therefore chosen for all the remaining calculations of this study.

Although this analysis was limited to Hartree–Fock calculations, we note that the basis set requirements of Hartree–Fock and DFT are known to be similar.¹²⁵ Furthermore, reliable reference energies for DFAs can be obtained with fully numerical methods,^{126–128} and exploratory calculations presented in the supplementary material confirm that the BSTEs in the AHGBSP3-9 basis are small also for DFAs.

B. OEE cation benchmark

1. Exploratory analysis

We begin the analysis by a graphical study of the results of the SPW92, PBEsol, revTPSS, MN15-L, BHandH and DM21 functionals in figure 2. This limited set of functionals contains LDA, GGA, and meta-GGA functionals from first principles (SPW92, PBEsol, and revTPSS, respectively), semiempirical functionals (MN15-L and DM21) as well as hybrid functionals (BHandH and DM21).

As will be discussed in section §III B 2, revTPSS is the most accurate meta-GGA functional for the $1s$ state. In figure 2, revTPSS is outperformed by DM21 only for He^+ , and otherwise revTPSS affords much lower errors than the five other functionals in the figure. In contrast, the performance of DM21 is inconsistent. DM21 has lower errors for light ions than for heavy ions, but the curve is kinked for the light ions. DM21’s curve becomes smooth for heavy ions, but DM21 is also less accurate for heavy ions. MN15-L also shows a kinky behavior with lower errors for light ions; these non-systematic features of DM21 and MN15-L can be tentatively explained by their semiempirical character; the curves for the first principles functionals are smoother.

The functional errors for the $2p$ state are shown in figure 2(b). The performance for the $2p$ state is strikingly different compared to the $1s$ state shown in figure 2(a). The plots for the $2p$ state in figure 2(b) show more structure and curve crossings. The behavior of

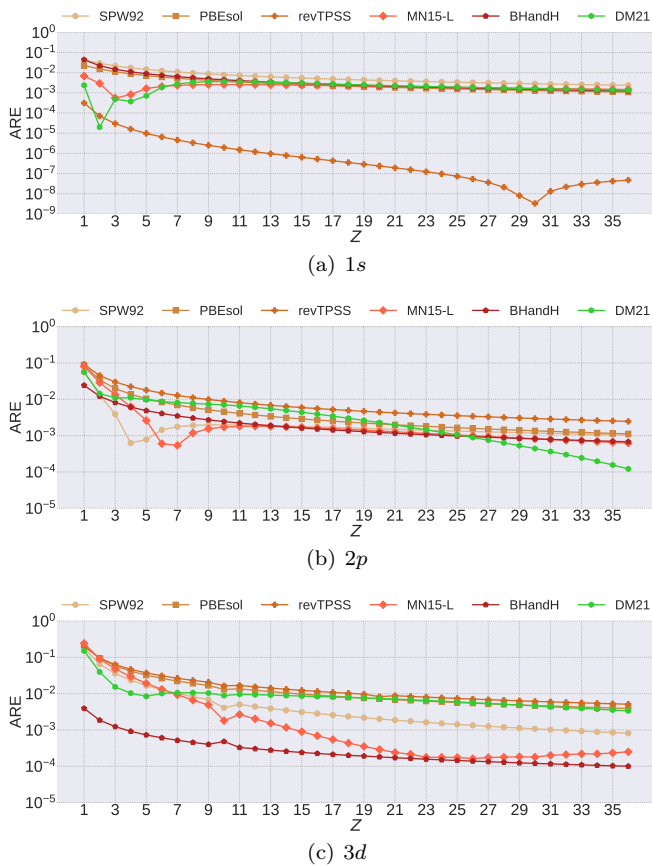


Figure 2. Functional errors for the $1s$, $2p$, and $3d$ states for the SPW92, PBEsol, revTPSS, MN15-L, BHandH, and DM21 functionals.

DM21 is qualitatively different from that of the other functionals: DM21 shows large relative errors for light atoms and lower relative errors for heavy atoms, while most of the other functionals shown behave similarly to each other. The only other exceptions to this are the SPW92 and MN15-L functionals that show dips at $Z \simeq 3$ and $Z \simeq 4$, respectively; the two functionals are thus oddly more accurate for some values of Z than others.

The errors for the $3d$ state are shown in figure 2(c). BHandH has small errors for all ions for the $3d$ state. The behavior of DM21 and MN15-L again differs qualitatively from the other functionals. While DM21 shows less variation for the $3d$ state than for the $2p$ state, MN15-L does the opposite: MN15-L has large errors for light ions, becomes nearly as accurate as BHandH for $Z \simeq 22$, while the relative error increases again for heavier ions.

2. Full analysis

The MSEs and OE for all studied functionals are shown in table 1. Although table 1 contains all of the data used in the present analysis, additional tables showing the rankings of the functionals in terms of the errors for

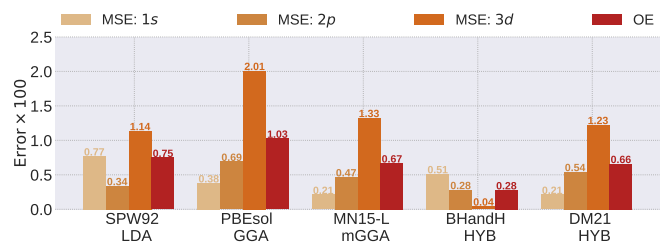


Figure 3. MSEs and OEs for the best functional of each rung of Jacob's ladder of all the investigated functionals.

the $1s$, $2p$ and $3d$ states as well as in terms of the overall error can be found in the supplementary material.

Clearly, the performance of all LDAs is practically identical. This suggests that the functional error for LDAs is limited by the simple functional form. While LDAs show larger errors than GGAs and meta-GGAs for the $1s$ state, they perform better than GGAs and meta-GGAs for the $2p$ and $3d$ states.

PBEsol¹⁰⁴ is the GGA that yields the smallest errors for the $2p$ and $3d$ states, as well as the smallest overall error. The XLYP GGA has a lower error than PBEsol for the $1s$ state. Although XLYP and even PBEsol are better for $1s$ states than any LDA, they have higher OEs than any LDA because of their considerably poorer performance for the $2p$ and $3d$ states. Analogous findings apply also to all other studied GGAs.

The best meta-GGA for the $1s$ state is revTPSS,^{99,100} closely followed by rSCAN,¹²¹ and r²SCAN¹¹⁸ (see table 1 or the supplementary material). The best meta-GGA in terms of overall error is MN15-L.⁹⁷

Hybrid functionals have better accuracy, as they contain some Hartree–Fock exchange which is free of self-interaction. The best hybrid GGA functionals in terms of overall error are BHandH⁷³ and QTP17.¹⁰⁹ BHandH has low MSEs for all states and has the best overall performance, which can be understood by its composition of 50% of Hartree–Fock exchange and 50% LDA exchange + 100% Lee–Yang–Parr correlation. QTP17 has the second best performance for all states; it, too, contains a mixture of Hartree–Fock (62%) and LDA exchange (38%).

The best functionals of each rung in terms of overall error are SPW92, PBEsol, MN15-L, and BHandH, respectively. The corresponding error distributions are summarized in comparison to DM21 in figure 3. Interestingly, the performance of the DM21 functional appears similar to that of MN15-L.

Following Medvedev *et al.*²⁷, the calculated OE for all functionals and ions is plotted against the publication year in figure 4. As is clear from this plot, the improvement in one-electron error is not fully systematic and features a significant amount of spread and some notable outliers like M11-L, GAM, and TASK. However, in the recent decade, hybrid functionals have become better overall. As an example, the various QTP functionals dominate the bottom right of the figure; these functionals are closely related in functional form and contain

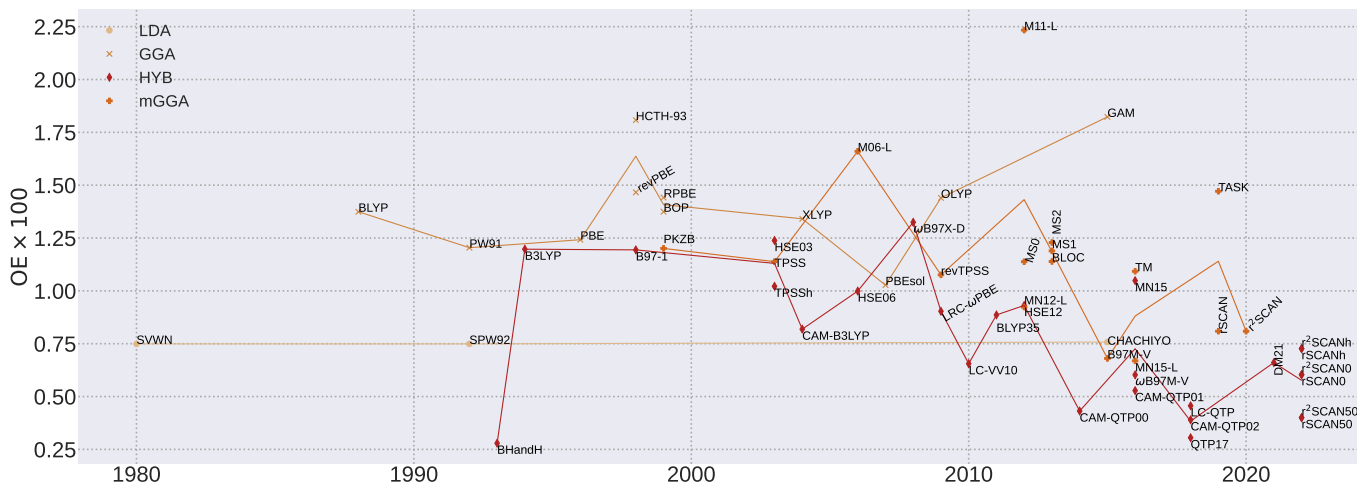


Figure 4. The overall functional error (OE) for various types of functionals, plotted as a function of the publication year. Yearly averages are shown as solid lines as a guide to the eye.

high amounts of Hartree–Fock exchange which decreases the one-electron error. Unsurprisingly, hybrid functionals based on rSCAN and r²SCAN perform well, and the functionals with large fractions of Hartree–Fock exchange share the bottom right of the figure with the QTP functionals.

3. Comparison to literature data

The study of Lonsdale and Goerigk⁵⁶ employed an uncontracted aug-cc-pVQZ basis set^{129,130} with the following nucleus dependent quadrature grids for the study of 1s states of hydrogenic cations: (45,770) for H and He, (50, 770) for Li–Ne, (55, 770) for Na–Ar and (60, 770) for K–Kr. However, it appears that K and Ca were excluded from Ref. 56 (see caption of Figs. 3 and 10 in Ref. 56).

Our trends and absolute values for the MSE for the 1s state are in satisfactory agreement for the subset of functionals studied in both works, although we did identify basis set incompleteness issues in some results of Ref. 56 as discussed in the supplementary material. The largest basis set incompleteness effects are observed for the M11-L and M06-L Minnesota functionals, which are known to converge remarkably slowly to the basis set limit.¹³¹

Lonsdale and Goerigk⁵⁶ only studied one LDA functional (SVWN); we considered more LDAs and found them to have similar performance. Lonsdale and Goerigk⁵⁶ found OLYP to be the best GGA functional for the 1s state; we also considered XLYP and found it to yield a considerably lower MSE for the 1s state than OLYP. Lonsdale and Goerigk⁵⁶ included a broader set of hybrid functionals separating global, range-separated hybrids and double hybrids; however, our main motivation is the connection to self-interaction corrected methods where hybrid functionals are typically not used. We found rSCAN50/r²SCAN50 to be the best hybrid functional for the 1s state, while Lonsdale and Go-

erigk⁵⁶ determined TPSSh and SCAN0 to be the best hybrids. All rSCAN and r²SCAN based hybrid functionals, i.e., rSCANh/r²SCANh, rSCAN0/r²SCAN0, and rSCAN50/r²SCAN50 as well as TPSSh have a good performance for the 1s state. The revTPSS functional is found in our work as well by Lonsdale and Goerigk⁵⁶ to be the best non-hybrid meta-GGA functional for the 1s state.

IV. SUMMARY AND DISCUSSION

We used exactly solveable hydrogenic cations in their 1s ground state and 2p and 3d excited states to determine the self-consistent one-electron error for 56 density functionals including the novel DM21 of Kirkpatrick *et al.*⁵⁸, employing the methodology of Gunnarsson and Lundqvist⁵⁷ for the excited state calculations. In accordance with an earlier finding by Sun *et al.*⁵⁴ apparently based on non-self-consistent calculations for the hydrogen atom and molecule and one LDA functional, we find for 36 hydrogenic cations that all LDAs perform better for the excited 2p and 3d states than any of the tested GGAs and meta-GGAs. The performance of various LDAs appears to be almost identical, as the calculated errors are nearly indistinguishable, suggesting that the errors are limited by the simple functional form used in LDAs. Sun *et al.*⁵⁴ pointed out that larger errors for excited states are a necessary consequence of orbital nodality.

The revTPSS functional is the best performing meta-GGA for the 1s state, tightly followed by the rSCAN and r²SCAN functionals. MN15-L shows a better overall performance than LDAs for all states; however, the performance of MN15-L is non-systematic like that of DM21.

Hybrid functionals like BHandH and QTP17 have the best overall performance as they explicitly include some fraction of Hartree–Fock exchange. Moreover, both

BHandH and QTP17 are mixtures of Hartree–Fock and LDA exchange, leading to the good observed accuracy.

DM21 turns out to be only close to exact for the 1s state OEE from H^0 to B^{4+} (see figure 2). For He^+ to B^{4+} DM21 shows also good performance for 2p and 3d states. However, over the whole range of investigated species H^0 to Kr^{35+} , DM21 exhibits various trend changes and an overall inconsistent performance. Thus, one might improve the next generation of the DM21 functional by including more one-electron cations in the training sets for various elements in the periodic table. This might increase the consistency of promising properties of such kind of machine-learned functionals.

We found PBEsol to be the most accurate GGA functional for the 2p and 3d states. PBEsol is also the most accurate GGA functional overall. These findings are interesting to contrast with that of Lehtola, Jónsson, and Jónsson⁴⁷, who showed that PBEsol is one of the few functionals whose accuracy improves when PZ-SIC is applied with complex orbitals. The development of novel DFAs with reduced one-electron error could therefore be useful for PZ-SIC calculations, as the reduced one-electron errors (equation (2)) would affect the numerics of the PZ correction (equation (1)) and might alleviate well-known issues with PZ-SIC and PZFLO-SIC discussed in section §I.

Note added in proof After the acceptance of this paper, we became aware of a preprint by Lonsdale and Goerigk¹³² that includes discussion on excited states of hydrogenic cations.

SUPPLEMENTARY MATERIAL

Exploratory finite element studies of basis set truncation errors in density functional calculations. Sorted rankings of the functionals by errors for the 1s, 2p and 3d states as well as the overall error. Bar plots of the errors for all studied functionals. Comparison of the 1s data to the study of Lonsdale and Goerigk⁵⁶ with additional basis set incompleteness studies. Tables of the calculated total energies for the 1s, 2p, and 3d states for all studied functionals.

AUTHOR DECLARATIONS

The authors have no conflicts to disclose.

ACKNOWLEDGMENT

We thank Jens Kortus for valuable comments on the manuscript. S. Schwalbe has been funded by the Deutsche Forschungsgemeinschaft (DFG, German Research Foundation) - Project ID 421663657 - KO 1924/9-2. This work is part of the OpenSIC project. We thank ZIH Dresden for computational time and support.

- ¹P. Hohenberg and W. Kohn, “Inhomogeneous electron gas,” *Phys. Rev.* **136**, B864–B871 (1964).
- ²W. Kohn and L. J. Sham, “Self-consistent equations including exchange and correlation effects,” *Phys. Rev.* **140**, A1133–A1138 (1965).
- ³A. D. Becke, “Perspective: Fifty years of density-functional theory in chemical physics,” *J. Chem. Phys.* **140**, 18A301 (2014).
- ⁴R. O. Jones, “Density functional theory: Its origins, rise to prominence, and future,” *Rev. Mod. Phys.* **87**, 897–923 (2015).
- ⁵N. Mardirossian and M. Head-Gordon, “Thirty years of density functional theory in computational chemistry: an overview and extensive assessment of 200 density functionals,” *Mol. Phys.* **115**, 2315–2372 (2017).
- ⁶L. Goerigk and N. Mehta, “A trip to the density functional theory zoo: Warnings and recommendations for the user,” *Aust. J. Chem.* **72**, 563 (2019).
- ⁷U. von Barth, “Basic density-functional theory—an overview,” *Phys. Scr.* **T109**, 9 (2004).
- ⁸A. J. Cohen, P. Mori-Sánchez, and W. Yang, “Challenges for density functional theory,” *Chem. Rev.* **112**, 289–320 (2012).
- ⁹S. Lehtola, C. Steigemann, M. J. T. Oliveira, and M. A. L. Marques, “Recent developments in LIBXC – a comprehensive library of functionals for density functional theory,” *SoftwareX* **7**, 1–5 (2018).
- ¹⁰J. P. Perdew, K. Burke, and M. Ernzerhof, “Generalized gradient approximation made simple,” *Phys. Rev. Lett.* **77**, 3865 (1996).
- ¹¹J. Tao, J. P. Perdew, V. N. Staroverov, and G. E. Scuseria, “Climbing the density functional ladder: Nonempirical meta-generalized gradient approximation designed for molecules and solids,” *Phys. Rev. Lett.* **91**, 146401 (2003).
- ¹²J. P. Perdew, J. Tao, V. N. Staroverov, and G. E. Scuseria, “Meta-generalized gradient approximation: Explanation of a realistic nonempirical density functional,” *J. Chem. Phys.* **120**, 6898 (2004).
- ¹³J. Sun, A. Ruzsinszky, and J. P. Perdew, “Strongly constrained and appropriately normed semilocal density functional,” *Phys. Rev. Lett.* **115**, 036402 (2015).
- ¹⁴P. J. Stephens, F. J. Devlin, C. F. Chabalowski, and M. J. Frisch, “Ab initio calculation of vibrational absorption and circular dichroism spectra using density functional force fields,” *J. Phys. Chem.* **98**, 11623 (1994).
- ¹⁵A. D. Becke, “Density-functional thermochemistry. V. Systematic optimization of exchange-correlation functionals,” *J. Chem. Phys.* **107**, 8554 (1997).
- ¹⁶F. A. Hamprecht, A. J. Cohen, D. J. Tozer, and N. C. Handy, “Development and assessment of new exchange-correlation functionals,” *J. Chem. Phys.* **109**, 6264 (1998).
- ¹⁷A. D. Boese, N. L. Doltsinis, N. C. Handy, and M. Sprik, “New generalized gradient approximation functionals,” *J. Chem. Phys.* **112**, 1670 (2000).
- ¹⁸Y. Zhao, N. E. Schultz, and D. G. Truhlar, “Exchange-correlation functional with broad accuracy for metallic and non-metallic compounds, kinetics, and noncovalent interactions,” *J. Chem. Phys.* **123**, 161103 (2005).
- ¹⁹Y. Zhao, N. E. Schultz, and D. G. Truhlar, “Design of density functionals by combining the method of constraint satisfaction with parametrization for thermochemistry, thermochemical kinetics, and noncovalent interactions,” *J. Chem. Theory Comput.* **2**, 364 (2006).
- ²⁰N. Mardirossian and M. Head-Gordon, “How accurate are the Minnesota density functionals for noncovalent interactions, isomerization energies, thermochemistry, and barrier heights involving molecules composed of main-group elements?” *J. Chem. Theory Comput.* **12**, 4303–4325 (2016).
- ²¹N. Mardirossian and M. Head-Gordon, “ ω B97X-V: A 10-parameter, range-separated hybrid, generalized gradient approximation density functional with nonlocal correlation, designed by a survival-of-the-fittest strategy,” *Phys. Chem. Chem. Phys.* **16**, 9904–9924 (2014).

- ²²N. Mardirossian and M. Head-Gordon, "Mapping the genome of meta-generalized gradient approximation density functionals: The search for B97M-V," *J. Chem. Phys.* **142**, 074111 (2015).
- ²³N. Mardirossian and M. Head-Gordon, " ω B97M-V: A combinatorially optimized, range-separated hybrid, meta-GGA density functional with VV10 nonlocal correlation," *J. Chem. Phys.* **144**, 214110 (2016).
- ²⁴K. Brown, Y. Maimaiti, K. Treppe, T. Bligaard, and J. Voss, "MCML: Combining physical constraints with experimental data for a multi-purpose meta-generalized gradient approximation," *J. Comput. Chem.* **42**, 2004–2013 (2021).
- ²⁵Z. M. Sparrow, B. G. Ernst, T. K. Quady, and R. A. DiStasio, "Uniting nonempirical and empirical density functional approximation strategies using constraint-based regularization," *J. Phys. Chem. Lett.* **13**, 6896–6904 (2022).
- ²⁶K. Treppe and J. Voss, "Data-driven and constrained optimization of semi-local exchange and nonlocal correlation functionals for materials and surface chemistry," *J. Comput. Chem.* **43**, 1104–1112 (2022).
- ²⁷M. G. Medvedev, I. S. Bushmarinov, J. Sun, J. P. Perdew, and K. A. Lyssenko, "Density functional theory is straying from the path toward the exact functional," *Science* **355**, 49–52 (2017).
- ²⁸K. P. Kepp, "Comment on "Density functional theory is straying from the path toward the exact functional"," *Science* **356**, 496 (2017).
- ²⁹M. G. Medvedev, I. S. Bushmarinov, J. Sun, J. P. Perdew, and K. A. Lyssenko, "Response to Comment on "Density functional theory is straying from the path toward the exact functional"," *Science* **356**, 496 (2017).
- ³⁰K. P. Kepp, "Energy vs. density on paths toward more exact density functionals," *Phys. Chem. Chem. Phys.* **20**, 7538–7548 (2018).
- ³¹N. Q. Su, Z. Zhu, and X. Xu, "Doubly hybrid density functionals that correctly describe both density and energy for atoms," *Proc. Natl. Acad. Sci. U. S. A.* **115**, 2287–2292 (2018).
- ³²Y. Wang, X. Wang, D. G. Truhlar, and X. He, "How well can the M06 suite of functionals describe the electron densities of Ne, Ne⁶⁺, and Ne⁸⁺?" *J. Chem. Theory Comput.* **13**, 6068–6077 (2017).
- ³³E. Sim, S. Song, and K. Burke, "Quantifying Density Errors in DFT," *J. Phys. Chem. Lett.* **9**, 6385–6392 (2018), arXiv:1809.10347.
- ³⁴A. J. Cohen, P. Mori-Sánchez, and W. Yang, "Fractional view of the exchange-correlation functional and derivative discontinuity in density functional theory," *Psi-k Scientific Highlight of the Month* **99** (2010).
- ³⁵K. R. Bryenton, A. A. Adeleke, S. G. Dale, and E. R. Johnson, "Delocalization error: The greatest outstanding challenge in density-functional theory," *WIREs Comput. Mol. Sci.*, e1631 (2022).
- ³⁶A. Ruzsinszky, J. P. Perdew, G. I. Csonka, O. A. Vydrov, and G. E. Scuseria, "Spurious fractional charge on dissociated atoms: Pervasive and resilient self-interaction error of common density functionals," *J. Chem. Phys.* **125**, 194112 (2006).
- ³⁷B. G. Johnson, C. A. Gonzales, P. M. W. Gill, and J. A. Pople, "A density functional study of the simplest hydrogen abstraction reaction. Effect of self-interaction correction," *Chem. Phys. Lett.* **221**, 100–108 (1994).
- ³⁸M.-C. Kim, E. Sim, and K. Burke, "Understanding and Reducing Errors in Density Functional Calculations," *Phys. Rev. Lett.* **111**, 073003 (2013), arXiv:1212.3054.
- ³⁹E. Sim, S. Song, S. Vuckovic, and K. Burke, "Improving results by improving densities: Density-corrected density functional theory," *J. Am. Chem. Soc.* **144**, 6625–6639 (2022).
- ⁴⁰J. L. Bao, Y. Wang, X. He, L. Gagliardi, and D. G. Truhlar, "Multiconfiguration pair-density functional theory is free from delocalization error," *The Journal of Physical Chemistry Letters* **8**, 5616–5620 (2017).
- ⁴¹J. L. Bao, L. Gagliardi, and D. G. Truhlar, "Self-Interaction Error in Density Functional Theory: An Appraisal," *J. Phys. Chem. Lett.* **9**, 2353–2358 (2018).
- ⁴²J. P. Perdew and A. Zunger, "Self-interaction correction to density-functional approximations for many-electron systems," *Phys. Rev. B* **23**, 5048–5079 (1981).
- ⁴³M. R. Pederson, R. A. Heaton, and C. C. Lin, "Local-density Hartree-Fock theory of electronic states of molecules with self-interaction correction," *J. Chem. Phys.* **80**, 1972 (1984).
- ⁴⁴S. Lehtola and H. Jónsson, "Variational, self-consistent implementation of the Perdew-Zunger self-interaction correction with complex optimal orbitals," *J. Chem. Theory Comput.* **10**, 5324–5337 (2014).
- ⁴⁵J. P. Perdew, A. Ruzsinszky, J. Sun, and M. R. Pederson, "Paradox of self-interaction correction: How can anything so right be so wrong?" *Adv. At. Mol. Opt. Phys.* **64**, 1–14 (2015).
- ⁴⁶S. Lehtola, M. Head-Gordon, and H. Jónsson, "Complex orbitals, multiple local minima, and symmetry breaking in Perdew-Zunger self-interaction corrected density functional theory calculations," *J. Chem. Theory Comput.* **12**, 3195–3207 (2016).
- ⁴⁷S. Lehtola, E. Ö. Jónsson, and H. Jónsson, "Effect of complex-valued optimal orbitals on atomization energies with the Perdew-Zunger self-interaction correction to density functional theory," *J. Chem. Theory Comput.* **12**, 4296–4302 (2016).
- ⁴⁸M. R. Pederson, A. Ruzsinszky, and J. P. Perdew, "Communication: Self-interaction correction with unitary invariance in density functional theory," *J. Chem. Phys.* **140**, 121103 (2014).
- ⁴⁹K. Treppe, S. Schwalbe, S. Liebing, W. T. Schulze, J. Kortus, H. Myneni, A. V. Ivanov, and S. Lehtola, "Chemical bonding theories as guides for self-interaction corrected solutions: Multiple local minima and symmetry breaking," *J. Chem. Phys.* **155**, 224109 (2021).
- ⁵⁰X. Cheng, Y. Zhang, E. Jónsson, H. Jónsson, and P. M. Weber, "Charge localization in a diamine cation provides a test of energy functionals and self-interaction correction," *Nat. Commun.* **7**, 11013 (2016).
- ⁵¹Y. Zhang, P. M. Weber, and H. Jónsson, "Self-Interaction Corrected Functional Calculations of a Dipole-Bound Molecular Anion," *J. Phys. Chem. Lett.* **7**, 2068–2073 (2016).
- ⁵²A. V. Ivanov, T. K. Ghosh, E. Ö. Jónsson, and H. Jónsson, "Mn dimer can be described accurately with density functional calculations when self-interaction correction is applied," *J. Phys. Chem. Lett.* **12**, 4240–4246 (2021).
- ⁵³E. Ö. Jónsson, S. Lehtola, and H. Jónsson, "Towards an Optimal Gradient-dependent Energy Functional of the PZ-SIC Form," *Procedia Comput. Sci.* **51**, 1858–1864 (2015).
- ⁵⁴J. Sun, J. P. Perdew, Z. Yang, and H. Peng, "Communication: Near-locality of exchange and correlation density functionals for 1- and 2-electron systems," *J. Chem. Phys.* **144**, 191101 (2016), arXiv:1603.04062.
- ⁵⁵C. Shahi, P. Bhattarai, K. Wagle, B. Santra, S. Schwalbe, T. Hahn, J. Kortus, K. A. Jackson, J. E. Peralta, K. Treppe, S. Lehtola, N. K. Nepal, H. Myneni, B. Neupane, S. Adhikari, A. Ruzsinszky, Y. Yamamoto, T. Baruah, R. R. Zope, and J. P. Perdew, "Stretched or nodded orbital densities and self-interaction correction in density functional theory," *J. Chem. Phys.* **150**, 174102 (2019).
- ⁵⁶D. R. Lonsdale and L. Goerigk, "The one-electron self-interaction error in 74 density functional approximations: a case study on hydrogenic mono- and dinuclear systems," *Phys. Chem. Chem. Phys.* **22**, 15805–15830 (2020).
- ⁵⁷O. Gunnarsson and B. I. Lundqvist, "Exchange and correlation in atoms, molecules, and solids by the spin-density-functional formalism," *Phys. Rev. B* **13**, 4274–4298 (1976).
- ⁵⁸J. Kirkpatrick, B. McMorro, D. H. Turban, A. L. Gaunt, J. S. Spencer, A. G. Matthews, A. Obika, L. Thiry, M. Fortunato, D. Pfau, *et al.*, "Pushing the frontiers of density functionals by solving the fractional electron problem," *Science* **374**, 1385–1389 (2021).
- ⁵⁹S. Lehtola and A. J. Karttunen, "Free and open source software for computational chemistry education," *Wiley Interdiscip. Rev.*

- Comput. Mol. Sci. **12**, e1610 (2022).
- ⁶⁰Q. Sun, X. Zhang, S. Banerjee, P. Bao, M. Barbry, N. S. Blunt, N. A. Bogdanov, G. H. Booth, J. Chen, Z.-H. Cui, J. J. Eriksen, Y. Gao, S. Guo, J. Hermann, M. R. Hermes, K. Koh, P. Koval, S. Lehtola, Z. Li, J. Liu, N. Mardirossian, J. D. McClain, M. Motta, B. Mussard, H. Q. Pham, A. Pulkin, W. Purwanto, P. J. Robinson, E. Ronca, E. R. Sayfutyarova, M. Scheurer, H. F. Schurkus, J. E. T. Smith, C. Sun, S.-N. Sun, S. Upadhyay, L. K. Wagner, X. Wang, A. White, J. D. Whitfield, M. J. Williamson, S. Wouters, J. Yang, J. M. Yu, T. Zhu, T. C. Berkelbach, S. Sharma, A. Y. Sokolov, and G. K.-L. Chan, "Recent developments in the Pyscf program package," *J. Chem. Phys.* **153**, 024109 (2020), arXiv:2002.12531.
- ⁶¹S. Lehtola, "Assessment of initial guesses for self-consistent field calculations. superposition of atomic potentials: Simple yet efficient," *J. Chem. Theory Comput.* **15**, 1593–1604 (2019), arXiv:1810.11659.
- ⁶²P. Pulay, "Convergence acceleration of iterative sequences. The case of SCF iteration," *Chem. Phys. Lett.* **73**, 393–398 (1980).
- ⁶³P. Pulay, "Improved SCF convergence acceleration," *J. Comput. Chem.* **3**, 556–560 (1982).
- ⁶⁴V. R. Saunders and I. H. Hillier, "A "Level-Shifting" method for converging closed shell Hartree–Fock wave functions," *Int. J. Quantum Chem.* **7**, 699–705 (1973).
- ⁶⁵S. Lehtola, "Polarized Gaussian basis sets from one-electron ions," *J. Chem. Phys.* **152**, 134108 (2020), arXiv:2001.04224.
- ⁶⁶F. Jensen, "Polarization consistent basis sets: Principles," *J. Chem. Phys.* **115**, 9113–9125 (2001).
- ⁶⁷F. Jensen, "Polarization consistent basis sets. III. The importance of diffuse functions," *J. Chem. Phys.* **117**, 9234–9240 (2002).
- ⁶⁸B. P. Pritchard, D. Altarawy, B. Didier, T. D. Gibson, and T. L. Windus, "New Basis Set Exchange: An open, up-to-date resource for the molecular sciences community," *J. Chem. Inf. Model.* **59**, 4814–4820 (2019).
- ⁶⁹J.-D. Chai and M. Head-Gordon, "Long-range corrected hybrid density functionals with damped atom-atom dispersion corrections," *Phys. Chem. Chem. Phys.* **10**, 6615–6620 (2008).
- ⁷⁰A. D. Becke, "Density-functional exchange-energy approximation with correct asymptotic behavior," *Phys. Rev. A* **38**, 3098 (1988).
- ⁷¹C. Lee, W. Yang, and R. G. Parr, "Development of the Colle–Salvetti correlation-energy formula into a functional of the electron density," *Phys. Rev. B* **37**, 785 (1988).
- ⁷²B. Miehlich, A. Savin, H. Stoll, and H. Preuss, "Results obtained with the correlation energy density functionals of Becke and Lee, Yang and Parr," *Chem. Phys. Lett.* **157**, 200 (1989).
- ⁷³A. D. Becke, "A new mixing of Hartree–Fock and local density-functional theories," *J. Chem. Phys.* **98**, 1372 (1993).
- ⁷⁴L. A. Constantin, E. Fabiano, and F. Della Sala, "Meta-GGA exchange-correlation functional with a balanced treatment of nonlocality," *J. Chem. Theory Comput.* **9**, 2256 (2013).
- ⁷⁵L. A. Constantin, E. Fabiano, and F. Della Sala, "Semilocal dynamical correlation with increased localization," *Phys. Rev. B* **86**, 035130 (2012).
- ⁷⁶M. Renz, K. Theilacker, C. Lambert, and M. Kaupp, "A reliable quantum-chemical protocol for the characterization of organic mixed-valence compounds," *J. Am. Chem. Soc.* **131**, 16292–16302 (2009).
- ⁷⁷M. Kaupp, M. Renz, M. Parthey, M. Stolte, F. Würthner, and C. Lambert, "Computational and spectroscopic studies of organic mixed-valence compounds: where is the charge?" *Phys. Chem. Chem. Phys.* **13**, 16973–16986 (2011).
- ⁷⁸T. Tsuneda, T. Suzumura, and K. Hirao, "A new one-parameter progressive Colle–Salvetti-type correlation functional," *J. Chem. Phys.* **110**, 10664 (1999).
- ⁷⁹T. Yanai, D. P. Tew, and N. C. Handy, "A new hybrid exchange-correlation functional using the Coulomb-attenuating method (CAM-B3LYP)," *Chem. Phys. Lett.* **393**, 51 (2004).
- ⁸⁰P. Verma and R. J. Bartlett, "Increasing the applicability of density functional theory. IV. Consequences of ionization-potential improved exchange-correlation potentials," *J. Chem. Phys.* **140**, 18A534 (2014).
- ⁸¹Y. Jin and R. J. Bartlett, "The QTP family of consistent functionals and potentials in Kohn–Sham density functional theory," *J. Chem. Phys.* **145**, 034107 (2016).
- ⁸²R. L. A. Haiduke and R. J. Bartlett, "Non-empirical exchange-correlation parameterizations based on exact conditions from correlated orbital theory," *J. Chem. Phys.* **148**, 184106 (2018).
- ⁸³P. A. M. Dirac, "Note on exchange phenomena in the Thomas atom," *Math. Proc. Cambridge Philos. Soc.* **26**, 376 (1930).
- ⁸⁴T. Chachiyo, "Simple and accurate uniform electron gas correlation energy for the full range of densities," *J. Chem. Phys.* **145**, 021101 (2016).
- ⁸⁵H. S. Yu, W. Zhang, P. Verma, X. He, and D. G. Truhlar, "Non-separable exchange-correlation functional for molecules, including homogeneous catalysis involving transition metals," *Phys. Chem. Chem. Phys.* **17**, 12146–12160 (2015).
- ⁸⁶J. Heyd, G. E. Scuseria, and M. Ernzerhof, "Hybrid functionals based on a screened Coulomb potential," *J. Chem. Phys.* **118**, 8207 (2003).
- ⁸⁷J. Heyd, G. E. Scuseria, and M. Ernzerhof, "Erratum: "Hybrid functionals based on a screened Coulomb potential" [*J. Chem. Phys.* **118**, 8207 (2003)]," *J. Chem. Phys.* **124**, 219906 (2006).
- ⁸⁸A. V. Krukau, O. A. Vydrov, A. F. Izmaylov, and G. E. Scuseria, "Influence of the exchange screening parameter on the performance of screened hybrid functionals," *J. Chem. Phys.* **125**, 224106 (2006).
- ⁸⁹J. E. Moussa, P. A. Schultz, and J. R. Chelikowsky, "Analysis of the Heyd–Scuseria–Ernzerhof density functional parameter space," *J. Chem. Phys.* **136**, 204117 (2012).
- ⁹⁰O. A. Vydrov and T. Van Voorhis, "Nonlocal van der Waals density functional: The simpler the better," *J. Chem. Phys.* **133**, 244103 (2010).
- ⁹¹M. A. Rohrdanz, K. M. Martins, and J. M. Herbert, "A long-range-corrected density functional that performs well for both ground-state properties and time-dependent density functional theory excitation energies, including charge-transfer excited states," *J. Chem. Phys.* **130**, 054112 (2009).
- ⁹²Y. Zhao and D. G. Truhlar, "A new local density functional for main-group thermochemistry, transition metal bonding, thermochemical kinetics, and noncovalent interactions," *J. Chem. Phys.* **125**, 194101 (2006).
- ⁹³Y. Zhao and D. G. Truhlar, "The M06 suite of density functionals for main group thermochemistry, thermochemical kinetics, noncovalent interactions, excited states, and transition elements: two new functionals and systematic testing of four M06-class functionals and 12 other functionals," *Theor. Chem. Acc.* **120**, 215 (2008).
- ⁹⁴R. Peverati and D. G. Truhlar, "M11-L: A local density functional that provides improved accuracy for electronic structure calculations in chemistry and physics," *J. Phys. Chem. Lett.* **3**, 117 (2012).
- ⁹⁵R. Peverati and D. G. Truhlar, "An improved and broadly accurate local approximation to the exchange-correlation density functional: The MN12-L functional for electronic structure calculations in chemistry and physics," *Phys. Chem. Chem. Phys.* **14**, 13171 (2012).
- ⁹⁶H. S. Yu, X. He, S. L. Li, and D. G. Truhlar, "MN15: A Kohn–Sham global-hybrid exchange-correlation density functional with broad accuracy for multi-reference and single-reference systems and noncovalent interactions," *Chem. Sci.* **7**, 5032–5051 (2016).
- ⁹⁷H. S. Yu, X. He, and D. G. Truhlar, "MN15-L: A new local exchange-correlation functional for Kohn–Sham density functional theory with broad accuracy for atoms, molecules, and solids," *J. Chem. Theory Comput.* **12**, 1280–1293 (2016).
- ⁹⁸J. Sun, B. Xiao, and A. Ruzsinszky, "Communication: Effect of the orbital-overlap dependence in the meta generalized gradient

- approximation," *J. Chem. Phys.* **137**, 051101 (2012).
- ⁹⁹J. P. Perdew, A. Ruzsinszky, G. I. Csonka, L. A. Constantin, and J. Sun, "Workhorse semilocal density functional for condensed matter physics and quantum chemistry," *Phys. Rev. Lett.* **103**, 026403 (2009).
- ¹⁰⁰J. P. Perdew, A. Ruzsinszky, G. I. Csonka, L. A. Constantin, and J. Sun, "Erratum: Workhorse semilocal density functional for condensed matter physics and quantum chemistry [Phys. Rev. Lett. 103, 026403 (2009)]," *Phys. Rev. Lett.* **106**, 179902 (2011).
- ¹⁰¹J. Sun, R. Haunschild, B. Xiao, I. W. Bulik, G. E. Scuseria, and J. P. Perdew, "Semilocal and hybrid meta-generalized gradient approximations based on the understanding of the kinetic-energy-density dependence," *J. Chem. Phys.* **138**, 044113 (2013).
- ¹⁰²N. C. Handy and A. J. Cohen, "Left-right correlation energy," *Mol. Phys.* **99**, 403 (2001).
- ¹⁰³J. P. Perdew, K. Burke, and M. Ernzerhof, "Errata: Generalized gradient approximation made simple [Phys. Rev. Lett. 77, 3865 (1996)]," *Phys. Rev. Lett.* **78**, 1396 (1997).
- ¹⁰⁴J. P. Perdew, A. Ruzsinszky, G. I. Csonka, O. A. Vydrov, G. E. Scuseria, L. A. Constantin, X. Zhou, and K. Burke, "Restoring the density-gradient expansion for exchange in solids and surfaces," *Phys. Rev. Lett.* **100**, 136406 (2008).
- ¹⁰⁵J. P. Perdew, S. Kurth, A. Zupan, and P. Blaha, "Accurate density functional with correct formal properties: A step beyond the generalized gradient approximation," *Phys. Rev. Lett.* **82**, 2544 (1999).
- ¹⁰⁶P. Ziesche and H. Eschrig, *Electronic Structure of Solids' 91: Proceedings of the 75. WE-Heraeus-Seminar and 21st Annual International Symposium on Electronic Structure of Solids Held in Gaussig (Germany), March 11-15, 1991*, Vol. 17 (De Gruyter Akademie Forschung, 1991).
- ¹⁰⁷J. P. Perdew, J. A. Chevary, S. H. Vosko, K. A. Jackson, M. R. Pederson, D. J. Singh, and C. Fiolhais, "Atoms, molecules, solids, and surfaces: Applications of the generalized gradient approximation for exchange and correlation," *Phys. Rev. B* **46**, 6671 (1992).
- ¹⁰⁸J. P. Perdew, J. A. Chevary, S. H. Vosko, K. A. Jackson, M. R. Pederson, D. J. Singh, and C. Fiolhais, "Erratum: Atoms, molecules, solids, and surfaces: Applications of the generalized gradient approximation for exchange and correlation," *Phys. Rev. B* **48**, 4978 (1993).
- ¹⁰⁹Y. Jin and R. J. Bartlett, "Accurate computation of x-ray absorption spectra with ionization potential optimized global hybrid functional," *J. Chem. Phys.* **149**, 064111 (2018).
- ¹¹⁰B. Hammer, L. B. Hansen, and J. K. Nørskov, "Improved adsorption energetics within density-functional theory using revised Perdew-Burke-Ernzerhof functionals," *Phys. Rev. B* **59**, 7413 (1999).
- ¹¹¹J. P. Perdew and Y. Wang, "Accurate and simple analytic representation of the electron-gas correlation energy," *Phys. Rev. B* **45**, 13244 (1992).
- ¹¹²F. Bloch, "Bemerkung zur Elektronentheorie des Ferromagnetismus und der elektrischen Leitfähigkeit," *Z. Phys.* **57**, 545 (1929).
- ¹¹³S. H. Vosko, L. Wilk, and M. Nusair, "Accurate spin-dependent electron liquid correlation energies for local spin density calculations: a critical analysis," *Can. J. Phys.* **58**, 1200 (1980).
- ¹¹⁴T. Aschebrock and S. Kümmel, "Ultranonlocality and accurate band gaps from a meta-generalized gradient approximation," *Phys. Rev. Res.* **1**, 033082 (2019).
- ¹¹⁵J. Tao and Y. Mo, "Accurate semilocal density functional for condensed-matter physics and quantum chemistry," *Phys. Rev. Lett.* **117**, 073001 (2016).
- ¹¹⁶V. N. Staroverov, G. E. Scuseria, J. Tao, and J. P. Perdew, "Comparative assessment of a new nonempirical density functional: Molecules and hydrogen-bonded complexes," *J. Chem. Phys.* **119**, 12129 (2003).
- ¹¹⁷X. Xu and W. A. Goddard, "The X3LYP extended density functional for accurate descriptions of nonbond interactions, spin states, and thermochemical properties," *Proc. Natl. Acad. Sci. U. S. A.* **101**, 2673 (2004).
- ¹¹⁸J. W. Furness, A. D. Kaplan, J. Ning, J. P. Perdew, and J. Sun, "Accurate and numerically efficient r²SCAN meta-generalized gradient approximation," *J. Phys. Chem. Lett.* **11**, 8208–8215 (2020).
- ¹¹⁹J. W. Furness, A. D. Kaplan, J. Ning, J. P. Perdew, and J. Sun, "Correction to "Accurate and numerically efficient r²SCAN meta-generalized gradient approximation"," *J. Phys. Chem. Lett.* **11**, 9248–9248 (2020).
- ¹²⁰M. Bursch, H. Neugebauer, S. Ehlert, and S. Grimme, "Dispersion corrected r²SCAN based global hybrid functionals: r²SCANh, r²SCAN0, and r²SCAN50," *J. Chem. Phys.* **156**, 134105 (2022).
- ¹²¹A. P. Bartók and J. R. Yates, "Regularized SCAN functional," *J. Chem. Phys.* **150**, 161101 (2019).
- ¹²²Y. Zhang and W. Yang, "Comment on "Generalized gradient approximation made simple"," *Phys. Rev. Lett.* **80**, 890 (1998).
- ¹²³J. P. Perdew and K. Schmidt, "Jacob's ladder of density functional approximations for the exchange-correlation energy," *AIP Conf. Proc.* **577**, 1–20 (2001).
- ¹²⁴A. D. Kaplan, B. Santra, P. Bhattarai, K. Wagle, S. T. ur Rahman Chowdhury, P. Bhetwal, J. Yu, H. Tang, K. Burke, M. Levy, and J. P. Perdew, "Simple hydrogenic estimates for the exchange and correlation energies of atoms and atomic ions, with implications for density functional theory," *J. Chem. Phys.* **153**, 074114 (2020).
- ¹²⁵K. A. Christensen and F. Jensen, "The basis set convergence of the density functional energy for H₂," *Chem. Phys. Lett.* **317**, 400–403 (2000).
- ¹²⁶S. Lehtola, "A review on non-relativistic, fully numerical electronic structure calculations on atoms and diatomic molecules," *Int. J. Quantum Chem.* **119**, e25968 (2019), arXiv:1902.01431.
- ¹²⁷S. Lehtola, "Fully numerical Hartree-Fock and density functional calculations. I. Atoms," *Int. J. Quantum Chem.* **119**, e25945 (2019), arXiv:1810.11651.
- ¹²⁸S. Lehtola, "Fully numerical calculations on atoms with fractional occupations and range-separated exchange functionals," *Phys. Rev. A* **101**, 012516 (2020), arXiv:1908.02528.
- ¹²⁹T. H. Dunning, "Gaussian basis sets for use in correlated molecular calculations. I. The atoms boron through neon and hydrogen," *J. Chem. Phys.* **90**, 1007 (1989).
- ¹³⁰R. A. Kendall, T. H. Dunning, and R. J. Harrison, "Electron affinities of the first-row atoms revisited. Systematic basis sets and wave functions," *J. Chem. Phys.* **96**, 6796 (1992).
- ¹³¹N. Mardirossian and M. Head-Gordon, "Characterizing and understanding the remarkably slow basis set convergence of several Minnesota density functionals for intermolecular interaction energies," *J. Chem. Theory Comput.* **9**, 4453–4461 (2013).
- ¹³²D. R. Lonsdale and L. Goerigk, "One-electron self-interaction error and its relationship to geometry and higher orbital occupation," (2022).